ELSEVIER

Journal of Nuclear Materials 258–263 (1998) 1979–1984

journal of nuclear materials

Hydrogen generation from steam reaction with tungsten

G.R. Smolik *, K.A. McCarthy, D.A. Petti, K. Coates

Idaho National Engineering and Environmental Laboratory/LMITCO, P.O. Box 1625, Idaho Falls, ID 83415, USA

Abstract

A LOCA in a fusion reactor involving an ingress of steam presents a safety concern due to hydrogen generated from steam reactions with plasma facing components. Hydrogen concentrations must be maintained below explosive levels. To support safety evaluations we have experimentally determined hydrogen generation rates when a tungsten alloy is exposed to steam from 400°C to 1200°C. We studied effects of steam pressure between 2.8×10^4 and 8.5×10^4 Pa, i.e., (0.28–0.84 atm) and gas velocity between 0.011 and 0.063 m/s. We present relationships for the reaction rates, oxidation phases, and mechanisms associated with the hydrogen generation.

1. Introduction

Tungsten as a heavy refractory metal retains properties to high temperatures and has low erosion making it a candidate for plasma facing components. Alloys of tungsten will become highly activated when exposed to high neutron fluences, and will form volatile oxide species in the presence of water. The volatilization mechanism has been studied at various water contents [1–3] and we have measured volatilization rates for dose calculations from mobilized activation products [4–6]. However, measurements of tungsten oxidation rates to provide hydrogen generation have been very limited. An earlier study [2] inferring oxidation rates from weight change are complicated by the volatilization process. Our previous estimates [7] of hydrogen generation rates were based upon measurements of alloy recession. We have performed this investigation to measure hydrogen generation directly using gas chromatography (GC). The hydrogen generation rates are examined with respect to temperature, steam pressure, and gas velocity.

2. Experimental procedures

The alloy used for this study was prepared from elemental powders. Rhenium and tantalum were used to simulate activated transmutation products and nickel and iron included to promote the sintering process. The resulting composition was (95.2 wt% W, 2.17 wt% Ni, 1.15 wt% Fe, 1.00 wt% Re, 0.10 wt% Cu, 0.165 wt% Co, 0.094 wt% Mn, and 0.093 wt% Ta). The powder mixture was cold isostatically pressed (CIPed) into a cylindrical form and sintered in a hydrogen atmosphere at 1500°C. Samples (3 mm thick) were cut from the final 16.3 −mm diameter cylinder. The samples having a nominal 5.6 $-cm^2$ surface area were ground to 600 grit, cleaned with acetone, and rinsed with ethanol.

The tests were performed in the set-up schematically shown in Fig. 1. Steam was generated and preheated in a tube furnace from a water input of 2 ml/min. This produced a steam flow of 2.5 l(STP)/min, which along with 12 ml/min of argon as a carrier gas, provided our baseline conditions of 8.5×10^4 Pa (0.84 atm) and 0.037 m/s gas velocity. Other flow rates of water and argon were used to vary steam pressure between 2.8×10^4 and 8.5×10^4 Pa and gas velocity between 0.011 and 0.063 m/s. The preheated gases flowed into a second tube furnace past the specimen. The specimen temperature was monitored with a thermocouple positioned directly above the specimen in the gas stream. The quartz test chamber had a 0.00113 m^2 cross section. The steam after flowing through a quartz wool filter to collect mobilized products was condensed out and residual gases collected and sampled with a gas chromatograph (GC).

The hydrogen measurements were converted to concentrations using calibrations established from standard mixtures of hydrogen and argon. These quantities were

* Corresponding author. Tel.: +1 208 526 8317; fax: +1 208 526 0690; e-mail: grs1@inel.gov.

0022-3115/98/$19.00
PII: S0022-3115(98)00169-X

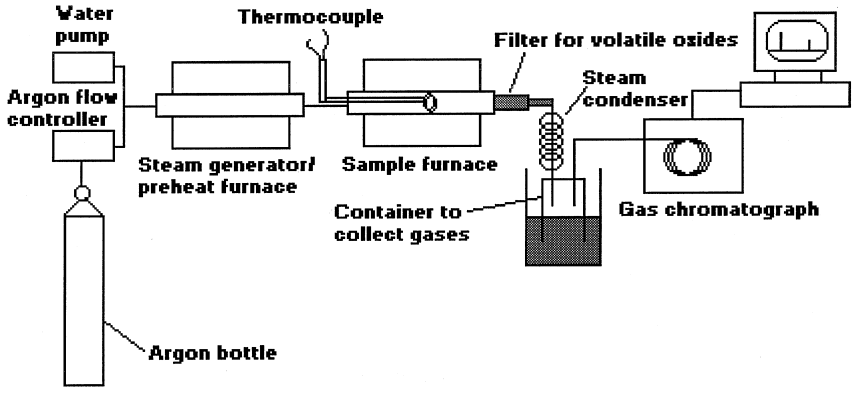

Fig. 1. Schematic of test system.

summed to provide cumulative plots for hydrogen generation. Posttest evaluations included mass change determinations and metallographic measurements of cross sections and oxide scale thicknesses. X-ray diffraction was performed on selected oxides from samples tested at 1000°C.

3. Experimental results and discussion

The cumulative hydrogen plots for various temperatures for the baseline condition of 8.5×10^4 Pa (0.84 atm) steam and 0.037 m/s are shown in Figs. 2 and 3. Linear oxidation kinetics prevail at 900°C, 1000°C, and 1200°C. Paralinear oxidation behavior occurred at lower temperatures. Fig. 2 shows that oxidation kinetics for W96-11 at 787°C over a longer time is generally linear. Even the parabolic behavior for the 500° and 650°C tests shown in Fig. 3 becomes more linear after 5 h. We have therefore calculated hydrogen generation rates (l/m^2 −s) assuming linear behavior. These rates, test conditions, and mass changes for all tests are summarized in Table 1.

We have plotted the hydrogen generation rates obtained at the various temperatures for the baseline condition with respect to reciprocal temperature (1/K) in Fig. 4. The data show a good fit to an Arrhenius relationship between 500°C and 1200°C. Eqs. (1) and (2) express the relationship with a coefficient of determination, r^2 of 0.997. No hydrogen signal was detectable with the GC during the 400°C test. We find that the detection limit, i.e., 3×10^{-7} l/m^2 −s, at 400°C lies near the extrapolation of the other data in Fig. 4.

$$\text{Rate}[\text{l H}_2(\text{STP})/\text{m}^2 - \text{s}] = 15,140\ [\exp(-16,720/\text{T})], \tag{1}$$

$$\text{Rate}(\text{kg H}_2/\text{m}^2 - \text{s}) = 1.3518[\exp(-16,720/\text{T})] \tag{2}$$

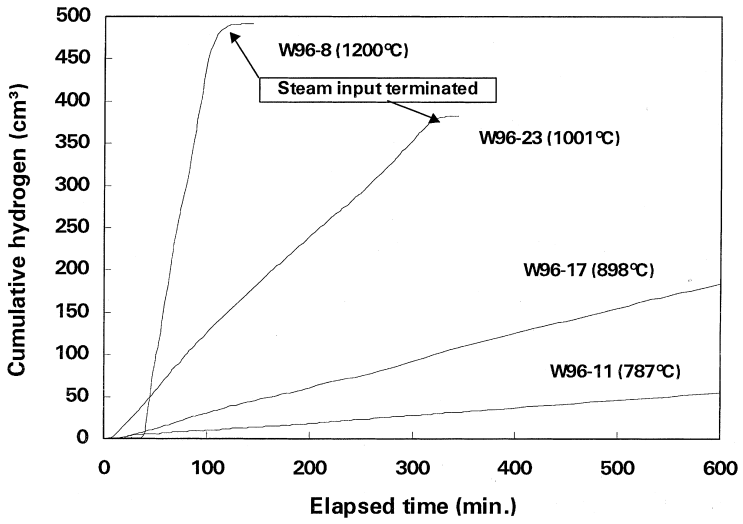

Fig. 2. Cumulative hydrogen plots for steam exposures near 800°C, 900°C, 1000°C and 1200°C.

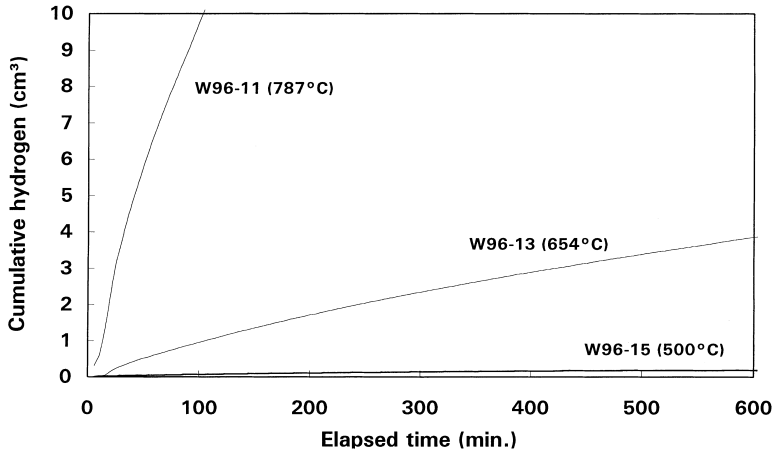

Fig. 3. Cumulative hydrogen plots for steam exposures near 500°C, 650°C and 780°C.

Table 1
Hydrogen generation rates and mass changes measured for steam tests

Specimen (I.D.)	Temperature (°C)/time (h)	Steam pressure Pa (atm)	Gas velocity, (m/s)	Steam/argon, (std cm³/min)	Hydrogen generation rate, (l (STP)/m² –s)	Mass change, (g)
W96-16	398/100	8.5×10^4 (0.84)	0.037	2500/12	0.0000003	n.d.
W96-15	500/100	8.5×10^4 (0.84)	0.037	2500/12	0.00000746	+0.0010
W96-13	654/20	8.5×10^4 (0.84)	0.037	2500/12	0.000153	+0.0034
W96-11	787/20	8.5×10^4 (0.84)	0.037	2500/12	0.002070	−0.0091
W96-9	800/20	8.5×10^4 (0.84)	0.037	2500/12	0.002310	−0.0751
W96-17	898/20	8.5×10^4 (0.84)	0.037	2500/12	0.007330	−0.4639
W96-8	1002/5	8.5×10^4 (0.84)	0.037	2500/12	0.0414	−0.4044
W96-27	999/5	2.8×10^4 (0.28)	0.011	250/490	0.0068	−0.0640
W96-29	998/5	4.3×10^4 (0.42)	0.011	370/380	0.0089	−0.1440
W96-28	1002/5	6.3×10^4 (0.62)	0.011	200/760	0.0105	−0.2185
W96-22	1000/5	8.2×10^4 (0.81)	0.012	746/32	0.0170	−0.3034
W96-23	1001/5	8.4×10^4 (0.83)	0.037	2500/32	0.0315	−0.4367
W96-30	1001/5	8.3×10^4 (0.82)	0.024	1620/35	0.0284	−0.5379
W96-31	991/5	8.4×10^4 (0.83)	0.063	4230/35	0.0450	−0.7256
W96-32	999/5	4.3×10^4 (0.42)	0.066	1870/2600	0.0192	−0.2602
W96-33	998/0.63	2.9×10^4 (0.29)	0.064	1260/3100	0.0297	−0.0364 [a]
W96-19	1200/1	8.5×10^4 (0.84)	0.037	2500/32	0.18573	−0.7035

[a] The test was prematurely terminated after 38 min.

Test parameters and data (linear hydrogen generation rates and mass changes) for tests conducted to evaluate influences of steam pressure and flow rate (gas velocity) are included in Table 1. These tests were run around 1000°C. To investigate the influence of steam pressure we held gas velocity constant, near 0.011 m/s, and varied steam pressure from 2.8×10^4 to 8.5×10^4 Pa. We found that the data were fairly linear on a log–log plot of rate versus steam pressure. A fit to the relationship of $\mathrm{Rate}[\mathrm{l\,H_2(STP)/m^2 - s}] = [0.0180] * \mathrm{P}^{(0.78)}$ was obtained with r^2 of 0.921. We again found an exponential relationship when steam was held near ambient pressure, i.e., 8.5×10^4 Pa (0.84 atm) and gas velocity varied from 0.011 to 0.063 m/s. The exponential relationship with a fit, r^2 equal to 0.981, was $\mathrm{Rate}[\mathrm{l\,H_2(STP)/m^2 - s}] = [0.00165] * V^{(0.56)}$. We have combined these observations into a general relationship shown by Eq. (3). The constant (1.02×10^5) has been derived for steam pressure expressed in units of (atm) and gas velocity as (m/s). We find that Eq. (3) predicts our experimentally derived data over all test conditions to within 35%. We recommend this relationship for conditions where flow behavior remains laminar.

$$\mathrm{Rate}[\mathrm{l\,H_2(STP)/m^2 - s}] = [1.02 \times 10^5] * [\mathrm{P}]^{(0.78)} * [\mathrm{V}]^{(0.56)} * [\exp(-16,720/\mathrm{T})]. \quad (3)$$

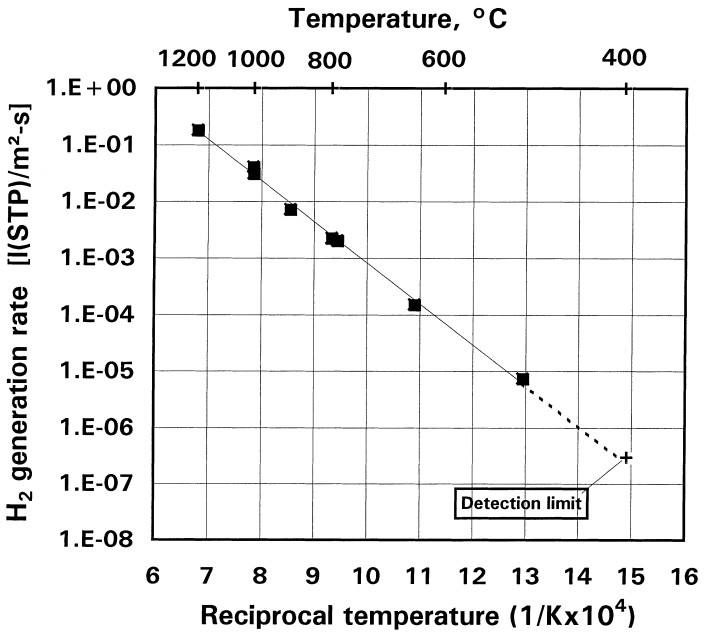

Fig. 4. Hydrogen generation rates plotted with respect to reciprocal temperature (1/K).

We observed that the sample tested at 400°C had only a slight bluish tint. Samples exposed at 500°C and 650°C had very adherent black oxide scales. Mass changes listed in Table 1 show that these specimens gained weight. Weight losses were recorded for all other specimens at higher temperatures showing effects of volatilization. All of the samples exposed at higher temperatures also had an outer layer of loose, porous black oxide. The thickness of the porous layer increased with higher steam pressure and gas velocity for the 1000°C exposures. The porous material could be easily removed revealing an underlying adherent bluish-black oxide scale. XRD analysis for samples exposed at 1000°C indicated that the loose, porous oxide was some form of mixed transition metal oxide-tungsten oxide such as $CoWO_4$ or $FeWO_4$. This phase, which incorporates some of the minor alloying elements apparently, is less volatile and remains on the specimen. XRD showed that the underlying adherent scale was predominantly WO_3 or $WO_{2.9}$. No evidence of WO_2 was found. The major phase that was found in mobilized products collected on the quartz wool filter was WO_3. There was some indications supporting the presence of a tungsten hydrogen oxide, $H_{0.23}WO_3$, but no evidence of

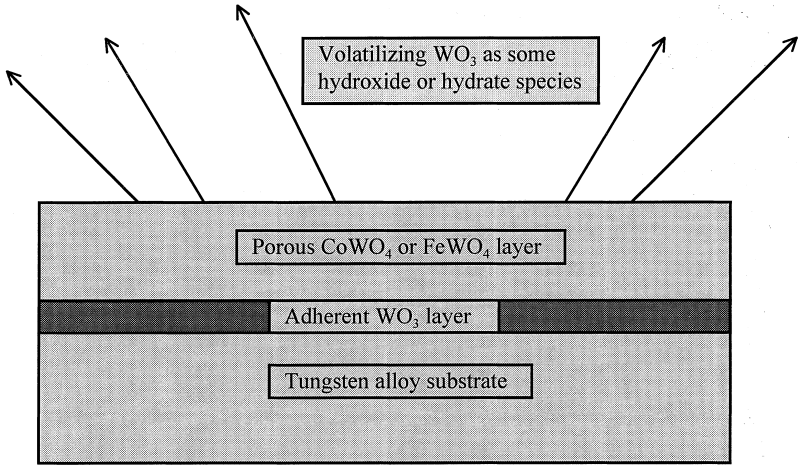

Fig. 5. Schematic of oxidation and volatilization processes.

any tungsten oxide hydroxides, i.e., either $WO_2(OH)_2$ or $W_6O_{16}(OH)$. This information supports the oxidation and volatilization processes schematically shown in Fig. 5. The lack of evidence for WO_2, from either the specimen or mobilized product, suggests that the volatilizing species is some hydroxide or hydrate complex of WO_3. This is in concurrence with the proposals by Battles, et al., [2] and Hastie [3]. This shows that all of the hydrogen comes from the oxidation process on the specimens and no additional hydrogen results from the volatilization process. Since only WO_3, or a near equivalent substoichiometric oxide, was found on the specimens essentially three moles of hydrogen are produced for each mole of tungsten oxidized.

Table 2
Hydrogen generation determined by various oxides (std cm^3) [a]

Specimen	Temperature, (°C)/time (h)	Steam pressure, Pa (atm)	Gas velocity (m/s)	H_2 determined from volatilized tungsten [b]	H_2 determined from porous oxide	H_2 determined from adherent oxide	H_2 measured with GC
W96-15	500/100	8.5×10^4(0.84)	0.037	1.4	–	1.5	1.8 [c]
W96-11	787/20	8.5×10^4(0.84)	0.037	24	16	64	84
W96-17	898/20	8.5×10^4(0.84)	0.037	203	39	87	355
W96-27	999/5	2.8×10^4(0.28)	0.011	36	16	37	77
W96-29	998/5	4.3×10^4(0.42)	0.011	71	21	55	100
W96-22	1000/5	8.2×10^4(0.81)	0.012	124	22	37	198
W96-23	1001/5	8.4×10^4(0.83)	0.037	177	32	47	377
W96-31	991/5	8.4×10^4(0.83)	0.063	281	45	32	485
W96-19	1200/1	8.5×10^4(0.84)	0.037	296	44	105	435

[a] Hydrogen calculations are based upon the reaction: $W + 3H_2O \rightarrow WO_3 + 3H_2$.
[b] Total volatilized tungsten is obtained from wight change plus oxygen in removable and anherent oxide.
[c] This amount is a linear projection based upon the amount measured during the first 10 h.

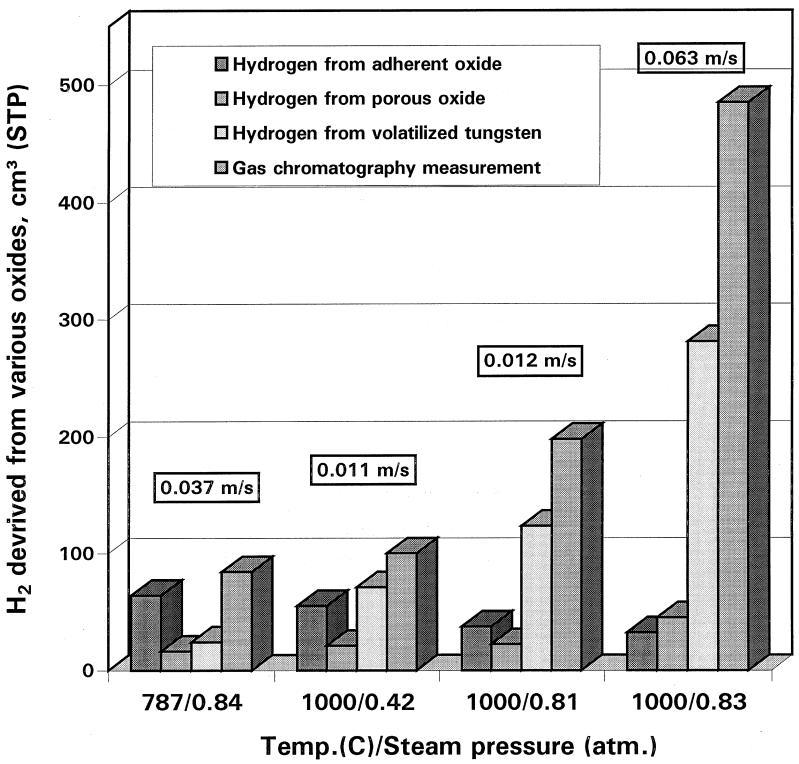

Fig. 6. Quantities of hydrogen determined from various types of oxides.

By using a combination of sample mass changes, mass of removable oxide, and thickness measurements of the residual adherent oxide we have calculated the amounts of hydrogen generated using: (1) the volatilized WO_3, (2) the loose, porous oxide, and (3) the adherent oxide scale. Data in Table 2 and the plots in Fig. 6 show how the hydrogen calculated from each type of oxide changes with temperature, steam pressure and flow rate. Most of the hydrogen is from the adherent oxide at low temperatures. The amounts of the volatilized WO_3 species increase with temperature, steam pressure, and flow rate. The plots in Fig. 6 reflect the increasing amounts and proportions of hydrogen determined from the volatilized oxide. We used these calculations to check our GC results. The sum of the hydrogen calculated for the three types of oxide always agreed within 35% of the cumulative hydrogen measurements from the GC.

4. Conclusions

We have observed in our test environments with high water vapor to hydrogen ratios that tungsten is essentially reacted to its highest oxidation state, i.e., WO_3. Basically three moles of hydrogen are formed for each mole of tungsten reacted. We did not find any evidence of WO_2. This reaffirms that the volatilizing species is some hydroxide or hydrate formed from the WO_3. No addition hydrogen results from the volatilization process. We find that hydrogen generation rates increase exponentially with steam pressure and gas velocity. We have derived Eq. (3) given below from direct hydrogen measurements with a GC to relate hydrogen generation rate to temperature, steam pressure, and gas velocity (for laminar flow). Temperature, steam pressure, and gas velocity for Eq. (3) are in units of kelvin (K), atmosphere (atm), and m/s, respectively.

$$\mathrm{Rate}[l\mathrm{H}_2(\mathrm{STP}).\mathrm{m}^2\ \mathrm{s}] = [1.02\times 10^5]* [P]^{(0.78)} * [V]^{(0.56)} * [\exp(-16,720/T)]. \quad (3)$$

Acknowledgements

This work is supported by the U.S. Department of Energy, Office of Energy Research, under DOE Idaho Operations Office Contract DE-AC07-94ID13223. This report is an account of work assigned to the US Home Team under Task Agreement No. S81-TT-08 within the Agreement among the European Atomic Energy Community, the Government of Japan, the Government of the Russian Federation, and the Government of the United States of America on Cooperation in the Engineering Design Activities for the International Thermonuclear Experimental Reactor "ITER EDA Agreement" under the auspices of the International Atomic Energy Agency (IAEA). This report has not been reviewed by the ITER Publications Office.

References

[1] O. Glemser, H.G. Wendlandt, Advan. Inorg. Chem. 5 (1963) 215.
[2] J.E. Battles, G.R.St. Pierre, R. Speiser, Metallurgie 7 (1967) 69.
[3] J.W. Hastie, High Temperature Vapors, Academic Press, New York, 1975, pp. 62–68.
[4] G.R. Smolik, S.J. Piet, R.M. Neilson Jr., Fusion Technol. 19 (1991) 1398.
[5] K.A. McCarthy, G.R. Smolik, S.L. Harms, A Summary and Assessment of Oxidation Driven Volatility Experiments at he INEL and Their Application to Fusion Reactor Safety, EGG-FSP-11193, September 1994.
[6] G.R. Smolik, K. Coates, Mobilization from Oxidation of a Tungsten Alloy in Steam, ITER/US/96/TE/SA-21, November 1996.
[7] G.R. Smolik, Tungsten Alloy Oxidation Behavior in Air and Steam, EGG-FSP-10166, March 1992.